ORIGINAL PAPER

A new transformation technique for evaluating nearly singular integrals

Wenjing Ye

Abstract Accurate evaluation of nearly singular integrals plays an important role in the overall accuracy of the Boundary Element Method (BEM). A new approach for the evaluation of nearly singular integrals particularly those with severe near singularity is described in this paper. This method utilizes a degenerate mapping to first reduce near singularity and then employs a variable transformation to further smooth out the resultant integrand. The accuracy and efficiency of the method are demonstrated through several examples that are commonly encountered in the applications of the BEM. Comparison of this method with some of the existing methods is also presented.

Keywords Nearly singular integrals ·
Numerical integration · Boundary element method ·
Non-linear variable transformation

1 Introduction

An important step in the implementation of the Boundary Element Method (BEM) is the evaluation of various integrals containing kernel functions of the type $O\left(1/r^\gamma\right)$, where r is the distance between the evaluation point (also called source point) and the field point. These integrals become singular or nearly singular when the source point collides with or is very close to the field point. Accurate evaluation of singular and nearly singular integrals plays a key role in the overall

W. Ye (✉)
Department of Mechanical Engineering,
Hong Kong University of Science and Technology,
Clear Water Bay, Kowloon, Hong Kong
e-mail: mewye@ust.hk

accuracy of the method because they are often the dominant components in the final discretized system.

It is well known that conventional Gaussian quadrature becomes inefficient or even inaccurate when applied to evaluate these integrals directly. Extensive research has been conducted to search for accurate and efficient methods. For singular integrals, the proposed methods include, but are not limited to, analytical and semi-analytical methods [10, 11,28], degenerate mappings [1,24], and various non-linear transformation techniques [20,22,31,32,35]. For nearly singular integrals, which sometimes are more difficult to compute, methods such as domain division [2,4,9,24], singularity subtraction [3], the line integral method for stress analysis of thin structures [27], a method based on continuous integral formulation for linear elasticity [29], and a variety of variable transformation techniques [5,7,12–19,21,23,25, 26,31–34] have been proposed. In the variable transformation techniques, nonlinear transformations are employed to smooth out the integrands before conventional Gaussian quadrature is applied. Impressive results obtained from these variable transformation techniques have been demonstrated on various examples. It is, however, difficult to find one particular method that is effective for a wide range of nearly singular integrals. In a recent study conducted by Johnston et al. [21], several variable transformation methods have been compared. It was concluded that the sinh transformation proposed by the authors of [21] was superior for a relatively large range of integrals with mild near singularity, while the $L_1^{-\frac{1}{5}}$ transformation [15] is the best for integrals with severe near singularity, i.e., when the source point is very close to the integration domain.

In this paper, a new approach based on variable transformations for evaluating nearly singular integrals with kernel type of $O\left(1/r^\gamma\right)$ is introduced. The aim of this work is at

developing a general method that is suitable for a wide range of nearly singular integrals. Particular focus is on integrals with severe near singularities, for example, near "hypersingular" integrals and beyond. In the sections that follow, a review of the existing variable transformation methods is given first, followed by the introduction of the new variable transformation method. Results on several 1-D and 2-D examples obtained from various methods are presented and compared next. Finally, a summary of the work is given in the last section.

2 Variable transformation techniques

The integrals considered in this work are of $O\left(1/r^{\gamma}\right)$ type, i.e., the integrands can be generalized as $f\left(r, \vec{x}\right)/r^{\beta}$, where $f \approx O\left(r^{\alpha}\right)$, $\gamma = \beta - \alpha \geq 1$ for surface integrals and $\gamma = \beta - \alpha \geq 2$ for volume integrals, $r = \|\vec{x} - \vec{x}_s\|$, $\vec{x} \in \Omega$, and $\vec{x}_s$ is the evaluation point that is located either very close to the integration domain Ω (nearly singular case) or inside the domain (singular case). In both cases, the direct application of numerical quadratures, such as Gaussian quadrature, for the evaluation of such integrals yields large errors. For weakly singular integrals, various forms of degenerate mappings have proven to be very effective in eliminating the singularity. When they are applied to nearly singular integrals, particularly when γ is large and/or r is small, the resultant integrands can still exhibit severe singular behavior as shown in the following analysis.

Consider a triangular element T shown in Fig. 1a, where $\vec{x}_s$ is the evaluation point and $\vec{x}_p$ is the closest point on the element to $\vec{x}_s$. Note $\vec{x}_p$ is not always the projection point of $\vec{x}_s$ on the element and it can locate either inside the domain or on one of the edges or vertices of the element. Based on the location of $\vec{x}_p$, the triangular element is then split into several subelements, each with $\vec{x}_p$ as one of its vertices (Fig. 1b). For example, if $\vec{x}_p$ locates inside the element, three subelements result. If $\vec{x}_p$ locates on one edge of the element, two subelements are sufficient. Consider the subelement, T', shown in Fig. 1c and let $\vec{x} = \eta_1 \vec{x}_1 + \eta_2 \vec{x}_2 + (1 - \eta_1 - \eta_2)\,\vec{x}_p$. This subelement is transformed into a rectangular triangle in a coordinate system described by (η_1, η_2) (Fig. 1d) and the corresponding integral is

$$\int_{T'} \frac{f\left(r, \vec{x}\right)}{r^{\beta}} dS\left(\vec{x}\right) = \iint_{T'} \frac{\tilde{f}\left(r, \eta_1, \eta_2\right)}{r^{\beta}} J_1\left(\eta_1, \eta_2\right) d\eta_1 d\eta_2, \tag{1}$$

where $r = \|\vec{x}_s - \vec{x}\| = \|\eta_1(\vec{x}_p - \vec{x}_1) + \eta_2(\vec{x}_p - \vec{x}_2) + (\vec{x}_s - \vec{x}_p)\|$ and J_1 is the Jacobian of the transformation.

Applying the degenerate mapping described in [1] and letting $\eta_1 = \rho \cos^2 \theta$ and $\eta_2 = \rho \sin^2 \theta$, the subelement T' is further transformed into a rectangle as illustrated in Fig. 1e.

The Jacobian of this transformation has a common factor, ρ. In weakly singular cases, this ρ cancels out the singular source, ρ, in the denominator and the resultant integrand becomes regular. In nearly singular cases, the original integral is transformed into

$$\int_{T'} \frac{f\left(r, \vec{x}\right)}{r^{\beta}} dS\left(\vec{x}\right)$$

$$= \int_0^{\frac{\pi}{2}} \int_0^1 \frac{\hat{f}\left(\rho, \theta, \vec{x}_s\right) \tilde{J}_1\left(\rho, \theta\right) \rho \sin 2\theta}{\left[d^2 + 2d\rho f_1\left(\theta\right) + \rho^2 f_2\left(\theta\right)\right]^{\beta/2}} d\rho d\theta, \tag{2}$$

where d is the distance between $\vec{x}_s$ and $\vec{x}_p$, $f_1\left(\theta\right) = \frac{(\vec{x}_s - \vec{x}_p)}{d} \cdot \left[\cos^2\left(\theta\right)\left(\vec{x}_p - \vec{x}_1\right) + \sin^2\left(\theta\right)\left(\vec{x}_p - \vec{x}_2\right)\right]$ and $f_2\left(\theta\right) = \cos^4\theta\left\|\vec{x}_p - \vec{x}_1\right\|^2 + 2\cos^2\theta\sin^2\theta\left(\vec{x}_p - \vec{x}_1\right) \cdot \left(\vec{x}_p - \vec{x}_2\right) + \sin^4\theta\left\|\vec{x}_p - \vec{x}_2\right\|^2$. A plot of the integrand as a function of ρ, at $\hat{f} = 1$, $\tilde{J}_1 = 1$, $\theta = \frac{\pi}{4}$, $f_1 = f_2 = 1$ and various d and β, reveals that this integral, although is not singular, exhibits singular behavior when d is small (Fig. 2). This singular behavior becomes more severe when β increases. Various variable transformations were proposed in the past to further regularize the integrand [17,26,33,34]. A common feature of such integrands is the coexistence of two vastly different scales. As shown in Fig. 2, the integrands are typically comprised of two regions: a fast changing region near $\rho = 0$ and a slowly varied region. Thus a good transformation technique would be the one that reduces the discrepancy between scales. This can be achieved by efficiently enlarging the fast varing region, thus more Gaussian points can be distributed in this region, and shrinking the slowly varing part. In the following sections, some existing variable transformation techniques in the literature are reviewed and a new method is presented next.

2.1 Existing variable transformation techniques

In this section, we review and analyze some existing variable transformation techniques by inspecting their transformation $(\rho - r)$ maps as well as the smoothness of the transformed integrands. As an example, the integral shown in the expression (3) with $\beta = 5$ and the evaluation point located at $\rho = -d$ is used as the model integral.

$$\int_0^1 \frac{\rho}{\left[d^2 + \rho^2\right]^{\beta/2}} d\rho \tag{3}$$

(a) Monomial polynomial transformations

As one of the pioneers in applying nonlinear transformation techniques to regularize weakly singular integrals and nearly singular integrals, Telles proposed a second-order and third-order polynomial transformations for nearly singular integrals [31,32]. When applied to the integral shown in (3),

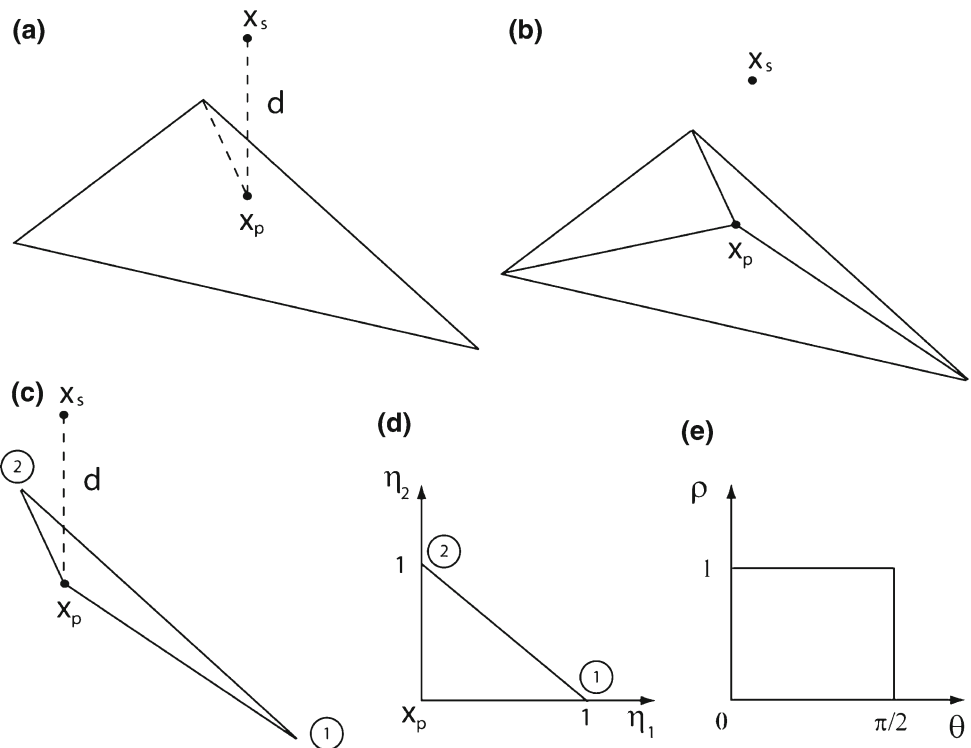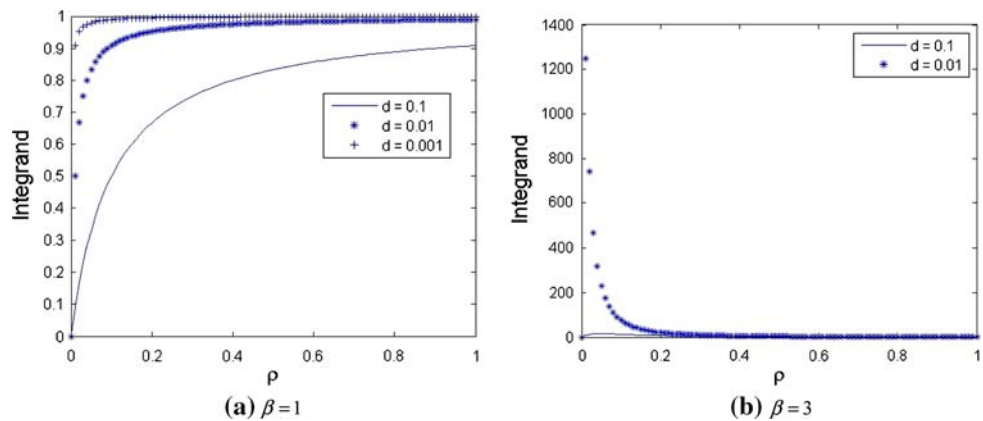**Fig. 1** Schematic of the
degenerate 2-D mapping

Fig. 2 Plots of an integrand as
a function of ρ: **a** $\beta = 1$,
b $\beta = 3$

(a) $\beta = 1$

(b) $\beta = 3$

Telles' transformations correspond to $\rho = r^2$ and $\rho = r^3$ respectively. A generalized form of this type of transformations is $\rho = r^m$ which maps $\rho \in [0, 1]$ to $r \in [0, 1]$. Such a transformation has been employed in [26]. Figure 3 shows the $\rho - r$ maps of this transformation corresponding to different m, from which it is clear that this transformation distributes more Gaussian points near the "singular" point, i.e., $\rho = 0$. But one drawback of such a transformation is that the effectiveness of this transformation is limited. This can be observed from Fig. 4 where the transformed integrands corresponding to the integral shown in (3) are plotted for different m and $d = 0.001$. It seems that the best transformation is the one corresponding to $m = 8$. Further increasing m would result in a decreasing efficiency because too many Gaussian points are clustered in a tiny region near the origin

and very few points are left for the rest of the domain. Even at $m = 8$, the transformed integrand is not as smooth as one would like to have, indicating further improvement may be possible.

(b) The "Huang–Cruse", "Wu" transformations

The "Huang–Cruse" transformation was proposed for evaluating nearly singular integrals in the form of $\int_0^a \frac{g(x)}{(xf(x)+d)^n} dx$, where $f(x)$ is a positive and slowly changing function within the integration interval [17]. The superior efficiency of this method was demonstrated on several examples. However, as pointed out by Wu [33], Huang and Cruse's method is only valid for certain cases. Their method was later extended by Wu and Lu for more general integrals [33,34]. For a detailed description of their methods, please refer to the papers [17,33,34].
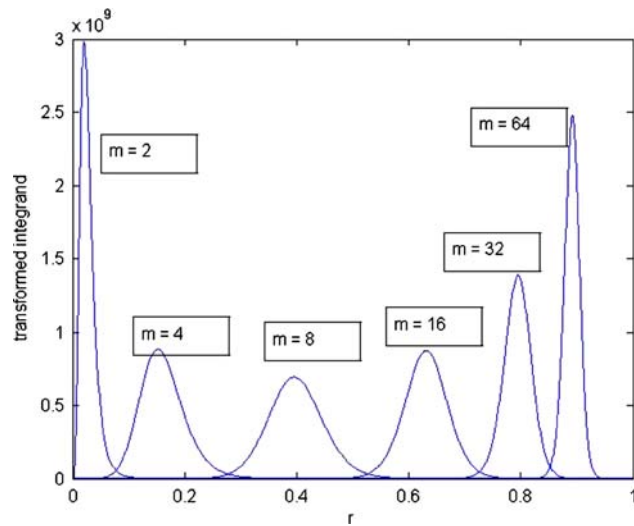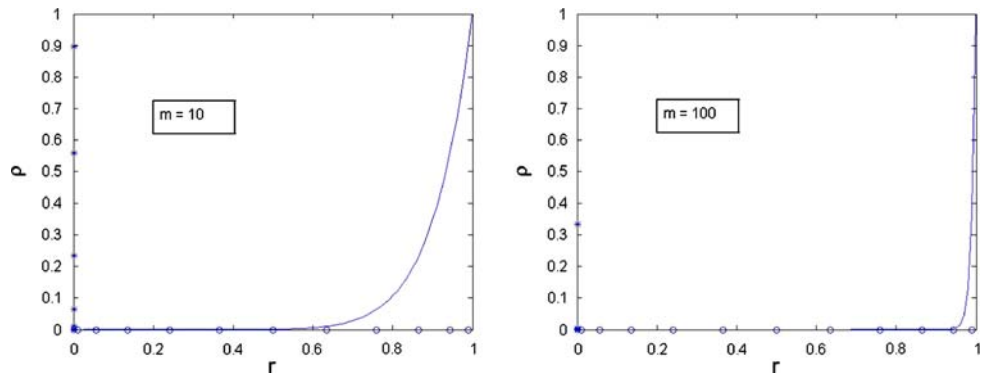
Fig. 4 The transformed integrands of the integral shown in (3) using $\rho = r^m$

(c) The PART method and the "L" transformations

In a series of papers published during 80's and 90's, the Projection and Angular and Radial Transformation (PART) method was introduced for the evaluation of nearly singular integrals [12–16]. Various radial transformations such as the "Log-L_1" transformation [12] and the $L^{-\frac{1}{5}}$ transformation [16] have been proposed to weaken the near singularity in the radial direction. According to [16], the $L^{-\frac{1}{5}}$ transformation performs the best among different L transformations for the calculation of nearly singular flux integrals.

Figure 5 shows the $\rho - r$ map of the $L^{-\frac{1}{5}}$ transformation and the transformed integrand corresponding to the model integral shown in (3). Comparing Fig. 5 with Figs. 3 and 4, one may conclude that the $L^{-\frac{1}{5}}$ transformation is more effective than the monomial polynomial transformations for the types of integrals similar to the model integral. One advantage of this transformation is that it incorporates the distance d into the transformation.

(d) Sigmoidal transformations (STs)

Sigmoidal transformations are a class of non-linear transformations that were initially proposed for evaluating singular integrals [6,8,19,30,35]. They can nevertheless also be applied to weaken near singularity and thus are useful for evaluating nearly singular integrals [18]. A common feature of various Sigmoidal transformations, such as the simple Sigmoidal transformation [6,8], the Sidi transformation [30], is that Gaussian points are clustered very fast towards the end points. For integrals with near singularity at only one end, semi-Sigmoidal transformations [19,23] are more effective than the classical Sigmoidal transformations. Figure 6 shows the $\rho - r$ map of the simple semi-Sigmoidal transformation, $\rho = \frac{2 \cdot (r/2)^m}{(r/2)^m + (1-r/2)^m}$ with $m = 3$, and the transformed integrand. One may conclude, based on the plots, that the effectiveness of the simple semi-Sigmoidal is similar to that of the monomial polynomial transformation with $m = 2$. Another popular Sigomoidal transformation is the Sidi transformation and the corresponding semi-Sidi transformation is $\rho = 2 \cdot \frac{\sqrt{\pi}\Gamma((m+1)/2)}{\Gamma(m/2)} \int_0^{r/2} (\sin \pi \xi)^{m-1} d\xi$. The effect of this transformation on reducing the near singularity is similar to that of the simple semi-Sigmoidal transformation.

(e) The sinh transformation

Following the notations used by Johnston et al. [21], the sinh transformation is described by the equations shown in (4).

$$s = s_0 + b \sinh (\mu_1 u - \eta_1)$$
$$t = t_0 + b \sinh (\mu_2 v - \eta_2) \tag{4}$$

where

$$\mu_1 = \frac{1}{2} \left[\text{arc sinh} \left(\frac{1 + s_0}{b} \right) + \text{arc sinh} \left(\frac{1 - s_0}{b} \right) \right],$$

$$\eta_1 = \frac{1}{2} \left[\text{arc sinh} \left(\frac{1 + s_0}{b} \right) - \text{arc sinh} \left(\frac{1 - s_0}{b} \right) \right],$$

$$\mu_2 = \frac{1}{2} \left[\text{arc sinh} \left(\frac{1 + t_0}{b} \right) + \text{arc sinh} \left(\frac{1 - t_0}{b} \right) \right],$$

$$\eta_2 = \frac{1}{2} \left[\text{arc sinh} \left(\frac{1 + t_0}{b} \right) - \text{arc sinh} \left(\frac{1 - t_0}{b} \right) \right],$$

Fig. 5 The $\rho - r$ map of the $L^{-\frac{1}{5}}$ transformation and the transformed integrand
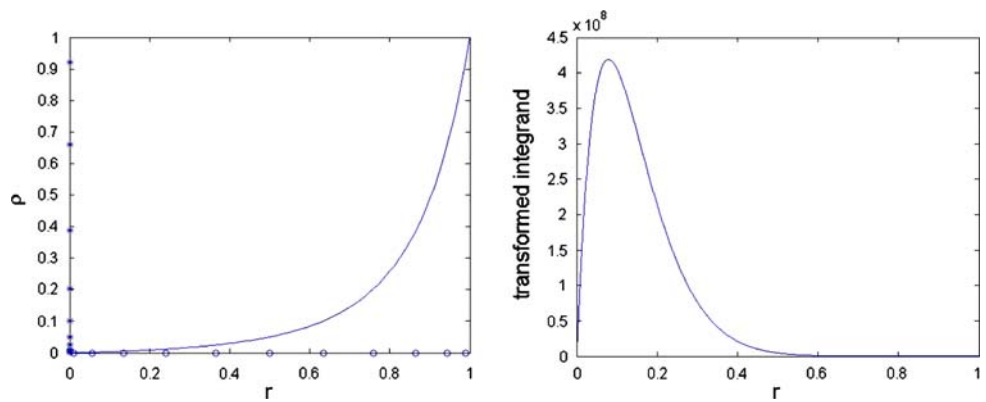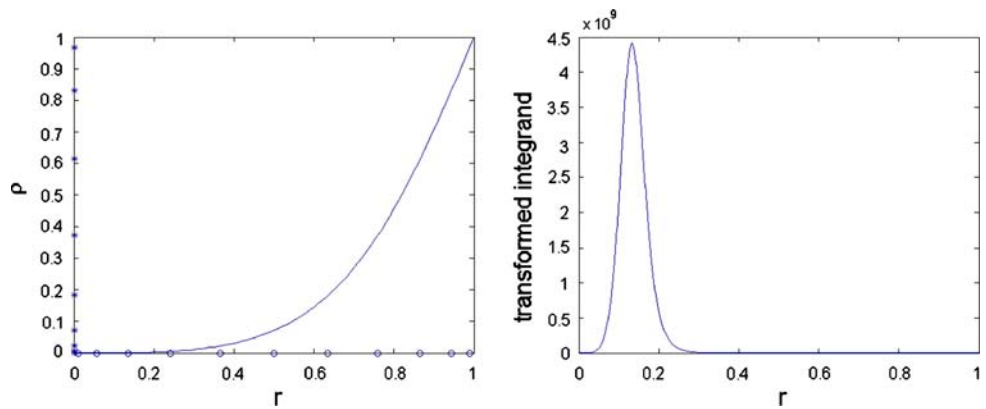

Fig. 6 *Left*: the $\rho - r$ map of the simple semi-Sigmoidal transformation ($m = 3$); *Right*: the transformed integrand

s_0, t_0 are the nearest point on the element to the evaluation point, b is the distance between them. This transformation maps $(s, t) \in [-1, 1]$ to $(u, v) \in [-1, 1]$. When applied to the model integral, the sinh transformation becomes $\rho = d$ sinh $\left(\text{arc sinh} \left(\frac{1}{d} \right) r \right)$. Figure 7 shows the $\rho - r$ map and the transformed integrand which are quite similar to that of Fig. 5. An advantage of this transformation is that it incorporates both the distance of the evaluation point to the element and the position of the projection of the source point.

2.2 New variable transformation technique

The proposed variable transformation is expressed in Eq. (5).

$$\rho = \frac{1}{m-1} \left(\frac{1 - r^m}{1 - r} - 1 \right), \tag{5}$$

where m is a parameter that can be chosen to suit for different level of near singularity. This transformation maps $\rho \in [0, 1]$ to $r \in [0, 1]$. Figure 8 shows the mapping and the distribution of Gaussian points in both domains for $m = 10$ and $m = 100$. Similar to most of the existing variable transformations, Gaussian points are clustered towards the singular point $\rho = 0$. But unlike the monomial polynomial transformations in which the map behaves more like a step function when m is large, this transformation distributes Gaussian

points more evenly which leads to a much smoother integrand after transformation as illustrated in Fig. 9. The motivation of the proposed variable transformation is based on the observation from Fig. 4 that for each different m, the corresponding monomial polynomial transformation shifts the "pulse" in the integrand, i.e. the source of near singularity initially located at $\rho = 0$, to a different location and at the same time, broadens the pulse to a certain extend. This naturally leads to the thought of that the sum of all these transformations would result in a much broader "pulse", i.e., a much smoother integrand. Equation (5) is equivalent to $\rho = \frac{\sum_{k=1}^{k=m-1} r^k}{m-1}$, which is the original form of the proposed transformation. However, Eq. (5) is recommended because it is much more computational efficient. It is also possible to derive several variations of (5) by assigning different weights to different orders of monomial polynomials, which may lead to better results in some cases.

3 Results and discussion

Several integrals are chosen to validate the accuracy as well as the efficiency of the proposed transformation technique for the evaluation of nearly singular integrals. For the one-dimensional integrals, results obtained from the proposed transformation with those obtained from the existing variable

Fig. 7 The $\rho - r$ map of the sinh transformation and the transformed integrand
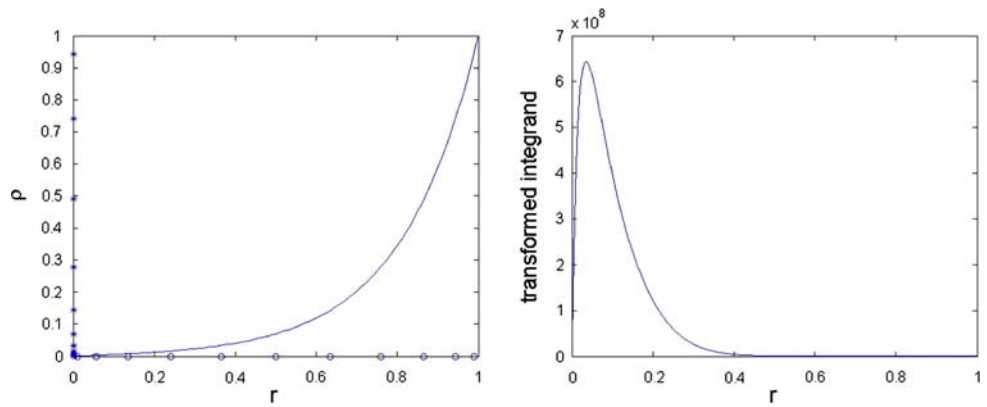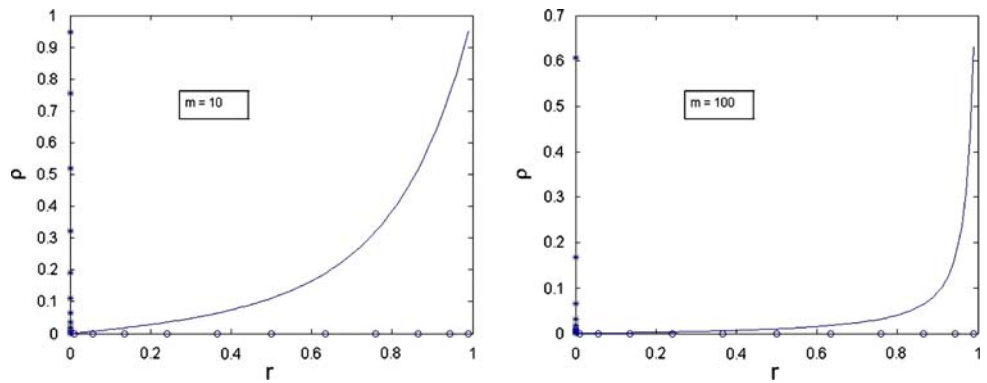

Fig. 8 Mapping between ρ and r, *circles* represent Gaussian points on $r \in [0, 1]$ and *stars* represent the corresponding points on ρ

transformation techniques are compared. In the two-dimensional example, the integration of $\frac{1}{r^\beta}$ on a square of $[-1, 1] \times [-1, 1]$ with the evaluation point located at various places is considered. This example was used in several references [17,26,33,34] in which methods such as the modified triangle polar co-ordinate mapping and the Huang–Cruse and the Wu's transformation techniques were employed. The results published in these references are used for comparison.

3.1 One-dimensional example

Consider one-dimensional integrals in the form of $\int_0^1 \frac{\rho}{[d^2 + f_1 \cdot 2d\rho + f_2 \cdot \rho^2]^{\beta/2}} d\rho$.

Based on the results presented in Tables 1, 2, 3 and 4, it is clear that the performances of the $L^{-\frac{1}{5}}$ transformation, the sinh transformation and the proposed transformation are far better than that of monomial polynomial transformations and various semi-Sigmoidal transformations. Among the three, it is noted that the performances of both the sinh transformation and the $L^{-\frac{1}{5}}$ transformation vary with the integrals, particularly when low-order Gaussian quadratures are employed. While the $L^{-\frac{1}{5}}$ transformation performs extremely well in case (4), its efficiency decreases when integrands vary slightly as shown in cases (1), (2) and (3). The sinh transformation, on the other hand, does very well in evaluating
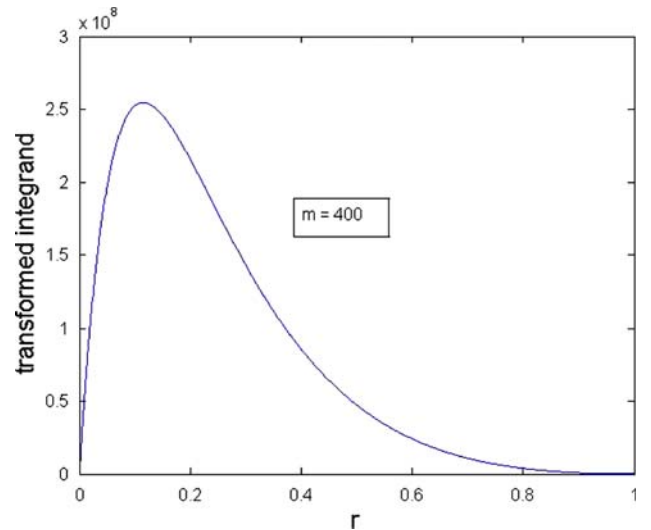
Fig. 9 The transformed integrand

integrals presented in cases (1) and (2), but not so well in cases (3) and (4). The proposed transformation, however, does very well for all the cases considered. This is largely attributed to the adjustable parameter, m. While it is usually regarded as a disadvantage to have a parameter in the formulation, in this case it is actually advantageous to have such an adjustable parameter which can be tuned to make the transformation optimal for a wide range of nearly singular integrals. This has been clearly demonstrated in the

Table 1 $\beta = 5$, $f_1 = 0$, $f_2 = 1$, $d = 0.01$, n: number of Gaussian points, exact solution: 333333.000049

		$n = 5$	$n = 10$	$n = 15$	$n = 20$
Monomial polynomial transformation	$m = 3$	472317.2156	318441.9470	333751.1105	333420.6197
	$m = 4$	283724.1253	375364.0461	338746.5625	333362.7874
	$m = 8$	488251.2222	357863.4595	316629.1402	335699.9242
$L^{-\frac{1}{5}}$ transformation		334704.6112	333430.6683	333332.1298	333333.0043
Simple semi-Sigmoidal transformation ($m = 3$)		445602.1808	361389.5263	331604.5568	333074.9740
Semi-Sidi transformation ($m = 5$)		188225.6464	382375.4884	349512.6276	335319.2399
Sinh transformation		313260.0940	333306.0462	333333.0107	333333.00007
Proposed transformation ($m = 50$)		336339.6843	333335.6640	333332.9968	333333.00003
Proposed transformation ($m = 100$)		334880.1271	333333.1649	333332.9839	333332.99882

Table 2 $\beta = 5$, $f_1 = 0$, $f_2 = 1$, $d = 0.001$, n: number of Gaussian points, exact solution: 333333333.000

		$n = 5$	$n = 10$	$n = 15$	$n = 20$
Monomial polynomial transformation	$m = 3$	80268938.67	275756303.2	326177863.9	333484116.5
	$m = 4$	135940040.4	490916778.8	297825887.4	332732841.6
	$m = 8$	65688215.50	478029462.0	382969658.5	325858474.9
$L^{-\frac{1}{5}}$ transformation		292823140.7	333815379.0	333338032.4	333333279.4
Simple semi-Sigmoidal transformation ($m = 3$)		41640433.56	337742755.2	361781499.9	335958058.9
Semi-Sidi transformation ($m = 5$)		36322299.08	301852015.1	309566829.9	347004108.0
Sinh transformation		320840548.6	333317475.2	333333501.1	333333334.1
Proposed transformation ($m = 400$)		339644063.5	333324116.5	333333341.8	333333333.8
Proposed transformation ($m = 800$)		331845860.7	333334079.6	333333329.0	333333332.8

Table 3 $\beta = 5$, $f_1 = 0.5$, $f_2 = 1.2$, $d = 0.001$, n: number of Gaussian points, exact solution: 130952865.897

		$n = 5$	$n = 10$	$n = 15$	$n = 20$
Monomial polynomial transformation	$m = 3$	62247503.87	141085813.7	138107729.7	132789155.0
	$m = 4$	50184983.89	174181537.0	129884258.9	129767759.3
	$m = 8$	27264838.66	150430192.5	142847011.2	131867026.6
$L^{-\frac{1}{5}}$ transformation		123772591.4	130935220.2	130952855.6	130952865.9
Simple semi-Sigmoidal transformation ($m = 3$)		20802996.09	115870547.3	133029376.1	131524187.3
Semi-Sidi transformation ($m = 5$)		119435703.6	150205027.9	118230688.9	134208728.9
Sinh transformation		145801573.2	130877957.5	130953111.3	130952865.2
Proposed transformation ($m = 800$)		130898582.2	130952864.9	130952863.2	130952865.7

Table 4 $\beta = 5$, $f_1 = 1$, $f_2 = 1$, $d = 0.001$, n: number of Gaussian points, exact solution: 83333333.0012

		$n = 5$	$n = 10$	$n = 15$	$n = 20$
Monomial polynomial transformation	$m = 3$	50532581.84	92168498.41	86372991.49	83668494.26
	$m = 4$	40411356.81	99673259.86	83959298.19	83158975.32
	$m = 8$	24944864.02	89584775.60	86389978.75	83591134.83
$L^{-\frac{1}{5}}$ transformation		83933407.59	83333333.00	83333333.00	83333333.00
Simple Semi-Sigmoidal transformation ($m = 3$)		19803076.55	75599328.32	83220877.20	83360491.40
Semi-Sidi transformation ($m = 5$)		83454287.81	95388152.00	78943505.28	83856747.53
Sinh transformation		93106638.35	83539570.48	83334541.69	83333337.55
Proposed transformation ($m = 800$)		83333347.25	83333332.73	83333328.89	83333332.76

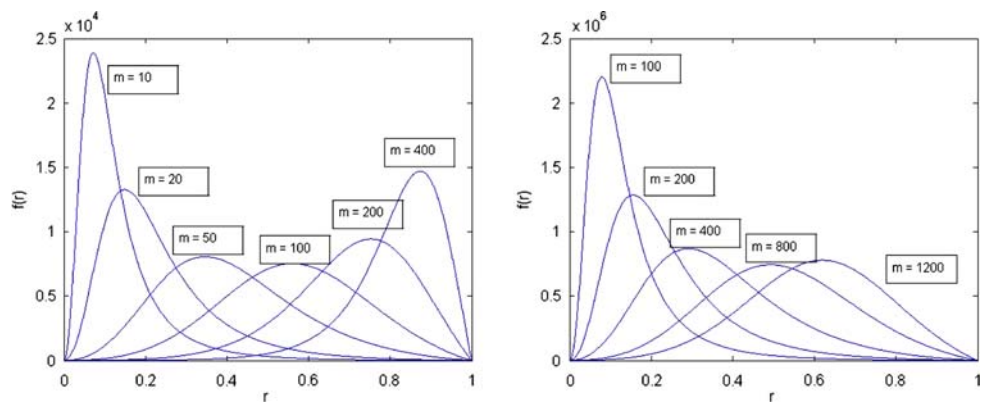**Fig. 10** The transformed integrands at different m

Table 5 Numerical results for $\beta = 3$, n is the total number of Gaussian points and the exact value is 5.20709224336

	$n = 6 \times 6$	$n = 10 \times 10$	$n = 15 \times 15$
Huang and Cruse's transformation [17]	5.20709226281	5.20709224335	NA
$L^{-\frac{1}{5}}$ transformation	5.20793150726	5.20709265930	5.20709224339
Sinh transformation	5.20709237304	5.20709224335	5.20709224335
Proposed transformation ($m = 10$)	5.20735170908	5.20709223291	5.20709224336

Table 6 Numerical results for $\beta = 5$, n is the total number of Gaussian points and the exact value is 51.5674930652

	$n = 6 \times 6$	$n = 10 \times 10$	$n = 15 \times 15$
Huang and Cruse's transformation	51.5674889113	51.5674930652	NA
$L^{-\frac{1}{5}}$ transformation	51.7633674951	51.5677884036	51.5674931112
Sinh transformation	51.5675379998	51.5674930621	51.5674930652
Proposed transformation ($m = 10$)	51.5687049270	51.5674930618	51.5674930653

results obtained. The key question is that how to select m for various different integrals. One approach is to employ a careful optimization process such as the one proposed by Telles in [31]. Another approach, despite its simplicity, has proved to be quite effective based on our experience. One can simply inspect the transformed integrands for various m and select the one that yields the smoothest integrand after transformation. Figure 10 shows the transformed integrands of the integrals considered in cases (1) and (2). Clearly for case (1), both $m = 50$ and $m = 100$ are good choices and for case (2), $m = 800$ is the best choice. These observations are indeed consistent with our results.

3.2 Two-dimensional example

$$I = \int_{\Omega} \frac{1}{r^{\beta}} dA, \quad \Omega \text{ is a square of } [-1, 1] \times [-1, 1].$$

(1) Evaluation point located at $(-1.1, -1.1, 0)$

This example was considered in references [17,26]. In reference [26], a modified triangle-polar coordinate mapping, which is equivalent to the degenerate mapping plus the monomial polynomial transformation mentioned above, was employed. Similar to the trend that was observed in the one-dimensional cases, this method is much less effective than some other transformations. Thus its results are not presented. Only those obtained from more effective transformations, i.e., the $L^{-\frac{1}{5}}$ transformation, the sinh transformation, the proposed transformation technique and the Huang and Cruse's transformation [17], are listed in Tables 5 and 6.

Based on the results shown in these tables, the most effective transformation for this case is the Huang and Cruse's transformation in which a 8/6-digit accuracy can be achieved by using only 6×6 Gaussian points. However, as pointed out by Wu [33], the Huang and Cruse's method, has certain limitation. For the case presented next, their method cannot be applied. For the other three transformations, while all of them produce almost the same results when $n \geq 15 \times 15$, the sinh transformation technique performs the best at low orders, followed by the proposed transformation technique. Note in the sinh transformation, there is no need to discretize the domain into triangles.

Table 7 Numerical results for $\beta = 5$, $d = 0.02848427$, exact solution is 92558.50373

	$n = 5 \times 5$	$n = 10 \times 10$	$n = 20 \times 20$	$n = 30 \times 30$	$n = 40 \times 40$
Huang–Cruse–Wu's transformation	NA	92550.513	92558.496	92558.496	92558.496
$L^{-\frac{1}{5}}$ transformation	95081	92555.93751	92558.50358	92558.50373	92558.50373
Sinh transformation	86836	92539.87605	92558.50368	92558.50373	92558.50373
Proposed transformation ($m = 30$)	93096	92553.68529	92558.50362	92558.50373	92558.50373

Table 8 Numerical results for $\beta = 5$, $d = 0.002848427$, exact solution is 92560071.88

	$n = 10 \times 10$	$n = 20 \times 20$	$n = 30 \times 30$	$n = 40 \times 40$
Huang–Cruse–Wu's transformation	92403606	92560120	92560131	92560132
$L^{-\frac{1}{5}}$ transformation	92603966.17	92560071.40	92560071.88	92560071.88
Sinh transformation	91371416.30	92559671.34	92560071.81	92560071.88
Proposed transformation ($m = 300$)	92555271.94	92560071.83	92560071.88	92560071.88

(2) Evaluation point located at $(0.0, 0.0, d)$

In references [33,34], Wu pointed out the limitation of Huang and Cruse's method and proposed several modifications so that this transformation method could be applied to more general integrals, i.e., to the cases when the closest point to the evaluation point locates inside the element. This was demonstrated by the same example that Huang and Cruse used but with the evaluation point located at $(0.0, 0.0, d)$, where d varies from 0.1414 to 0.002828427, corresponding to a d/D, D is the diagonal of the panel, of 5–0.1% respectively. Such integrals were also evaluated using other variable transformation methods. Results together with Wu's best results obtained from Eq. (20) in [34] are presented in Tables 7 and 8. For a concise presentation, only cases with severe near singularity are shown. For mild near singularity, for example, cases with $d/D = 5\%$ and $d/D = 2\%$, the trend is similar to that of the previous example.

Based on the results presented in the above tables, we found that the performance of the proposed transformation was better than that of the $L^{-\frac{1}{5}}$ transformation and the sinh transformation, particularly when low-order Gaussian quadrature was employed. When the order of Gaussian quadrature increases to a certain level ($n > 20$), all three transformations produce almost identical results. The accuracy and the efficiency of the Huang–Cruse–Wu's transformation at low-order Gaussian quadratures are comparable to that of the proposed transformation. However, it is observed the results from their transformation seem to converge to a set of values that are not consistent with the exact solutions presented in the tables.

4 Conclusions

A new approach is proposed as an alternative method for evaluating nearly singular integrals particularly for those with severe near singularity. This approach utilizes one form of the degenerate mapping to first reduce the near singularity and then to further smooth out the integrand by a variable transformation. Such a method is valid for both 1-D and 2-D integrals and can be easily extended to nearly singular volume integrals.

The accuracy and efficiency of the method was tested on several examples and compared with some existing methods. It has been found that the performance of the proposed method is relatively kernel independent, owing to an adjustable parameter in the formulation, while the performances of some other transformation based methods vary with the kernels. It has also been found for some mild nearly singular integrals considered, the sinh transformation outperforms the proposed method and others. However, for severe nearly singular cases, the proposed method is the best, particularly when low-order Gaussian quadratures ($n \leq 10$) are employed.

References

1. Anantharaman N, Mukherjee S (1993) A mapping method for numerical evaluation of two-dimensional integrals with 1/r singularity. Comput Mech 12:19–26
2. Banerjee PK, Wilson RB, Miller N (1985) Development of a BEM large system for three-dimensional inelastic analysis. In: Cruse TA (ed) Proc. ASME Conf. advanced topics in boundary element analysis. ASME, New York, pp 1–20
3. Cruse TA, Aithal R (1993) Non-singular boundary integral equation implementation. Int J Numer Methods Eng 36:237–254
4. Dallner R, Gunther K (1993) Efficient evaluation of volume integrals in the boundary element method. Comput Methods Appl Mech Eng 109:95–109
5. Duffy MG (1982) Quadrature over a pyramid or cube of integrands with a singularity at a vertex. SIAM J Numer Anal 9(6):1260–1262

6. Elliott D (1998) Sigmoidal transformation and the trapezoidal rule. J Aust Math Soc Ser B 40:E77–E137
7. Elliott D, Johnston PR (2007) Error analysis for a sinh transformation used in evaluating nearly singular boundary element integrals. J Comp Appl Math 203:103–124
8. Elliott D, Prössdorf S (1995) An algorithm for the approximate solution of integral equations of Mellin type. Numerische Mathematik 70:427–452
9. Gao XW, Davies TG (2002) Boundary element programming in mechanics. Cambridge University Press, Cambridge
10. Gray LJ, Martha LF, Ingraffea AR (1990) Hypersingular integrals in boundary element fracture analysis. Int J Numer Methods Eng 29:1135–1158
11. Guiggiani M (1991) The evaluation of Cauchy principal value integrals in the boundary element method—a review. Math Comput Model 15:175–184
12. Hayami K (1990) A robust numerical integration method for three dimensional boundary element analysis. In: Tanaka M, Brebbia CA, Honma T (ed) Boundary elements XII., vol 1. Computational Mechanics Publication, Southhampton, Springer, Berlin, pp 33–51
13. Hayami K (1992) A projection transformation method for nearly singular surface boundary element integrals. In: Breddia CA, Orszag SA (eds) Lecture Notes in Engineering, vol 73. Springer, Berlin
14. Hayami K (2005) Variable transformations for nearly singular integrals in the boundary element method. Publ RIMS, Kyoto Univ 41:821–842
15. Hayami K, Brebbia CA (1988) Quadrature methods for singular and nearly singular integrals in 3-D boundary element method. In: Brebbia CA (ed) Boundary elements X., vol 1, Southhampton, Springer, Berlin, pp 237–264
16. Hayami K, Matsumoto H (1994) A numerical quadrature for nearly singular boundary element integrals. Eng Anal Bound Elem 13:143–154
17. Huang Q, Cruse TA (1993) Some notes on singular integral techniques in boundary element analysis. Int J Numer Methods Eng 36:2643–2659
18. Johnston PR (1999) Application of sigmoidal transformations to weakly singular and near-singular boundary element integrals. Int J Numer Methods Eng 45:1333–1348
19. Johnston PR (2000) Semi-sigmoidal transformations for evaluating weakly singular boundary element integrals. Int J Numer Methods Eng 47:1709–1730
20. Johnston BM, Johnston PR (2003) A comparison of transformation methods for evaluating two-dimensional weakly singular integrals. Int J Numer Methods Eng 56:589–607
21. Johnston BM, Johnston PR, Elliott D (2007) A sinh transformation for evaluating two-dimensional nearly singular boundary element integrals. Int J Numer Methods Eng 69:1460–1479
22. Johnston PR, Elliott D (2001) A generalization of Telles' method for evaluating weakly singular boundary element integrals. J Comp Appl Math 131:223–241
23. Johnston PR, Elliott D (2002) Transformations for evaluating singular boundary element integrals. J Comp Appl Math 146:231–251
24. Lachat JC, Watson JO (1976) Effective numerical treatment of boundary integral equations: A formulation for three-dimensional elastostatics. Int J Numer Methods Eng 10:991–1005
25. Li HB, Han GM, Mang HA (1985) A new method for evaluating singular integrals in stress analysis of solids by the direct boundary element method. Int J Numer Methods Eng 21:2071–2098
26. Li Y, Obata T, Koguchi H, Yada T (1992) Some improvements of accuracy and efficiency in three dimensional direct boundary element method. Int J Numer Methods Eng 33:1451–1464
27. Liu Y (1998) Analysis of shell-like structures by the boundary element method based on 3-D elasticity: formulation and verification. Int J Numer Methods Eng 41:541–558
28. Moore MN, Gray LJ, Kaplan T (2007) Evaluation of supersingular integrals: Second-order boundary derivatives. Int J Numer Methods Eng 69:1930–1947
29. Mukherjee S, Chati MK, Shi X (2000) Evaluation of nearly singular integrals in boundary element contour and node methods for three-dimensional linear elasticity. Int J Solids Struct 37:7633–7654
30. Sidi A (1993) A new variable transformation for numerical integration. In: Brass H, Hämmerlin G (ed) Numerical integration IV. Birkhäuser, Basel, pp 359–373
31. Telles JCF (1987) A self-adaptive co-ordinate transformation for efficient numerical evaluation of general boundary element integrals. Int J Numer Methods Eng 24:959–973
32. Telles JCF, Oliveira RF (1994) Third degree polynomial transformation for boundary element integrals: further improvements. Eng Anal Bound Elem 13:135–141
33. Wu S (1995) On the evaluation of nearly singular kernel integrals in boundary element analysis. Numer Method Eng 11:331–337
34. Wu S, Lu P-A (1996) On the evaluation of nearly singular kernel integrals in boundary element analysis—some improved formulations. Comm Numer Method Eng 12:85–93
35. Yun BI (2006) A generalized non-linear transformation for evaluating singular integrals. Int J Numer Methods Eng 65:1947–1969